analytical chemistry

Article

Cite This: Anal. Chem. XXXX, XXX, XXX−XXX

pubs.acs.org/ac

Reactive Olfaction Ambient Mass Spectrometry

Dmytro S. Kulyk, Taghi Sahraeian, Qiongqiong Wan, and Abraham K. Badu-Tawiah*

Department of Chemistry and Biochemistry, The Ohio State University, 100 W. 18th Avenue, Columbus, Ohio 43210, United States

Supporting Information

ABSTRACT: Chemical ionization of organic compounds with negligible vapor pressures (VP) is achieved at atmospheric pressure when the proximal sample is exposed to corona discharge. The vapor-phase analyte is produced through a reactive olfaction process, which is determined to include electrostatic charge induction in the proximal condensed-phase sample, resulting in the liberation of free particles. With no requirement for physical contact, a new contained nano-atmospheric pressure chemical ionization (nAPCI) source was developed that allowed direct mass spectrometry analysis of complex mixtures at a sample consumption rate less than nmol/min. The contained nAPCI source was applied to analyze a wide range of samples including the detection of 1 ng/mL cocaine in serum and 200 pg/mL caffeine in raw urine, as well as the differentiation of chemical composition of perfumes and beverages. Polar (e.g., carminic acid; estimated VP 5.1×10^{-25} kPa) and nonpolar (e.g., vitamin D2; VP 8.5×10^{-11} kPa) compounds were successfully ionized by the contained nAPCI ion source under ambient conditions, with the corresponding ion types of 78 other organic compounds characterized.

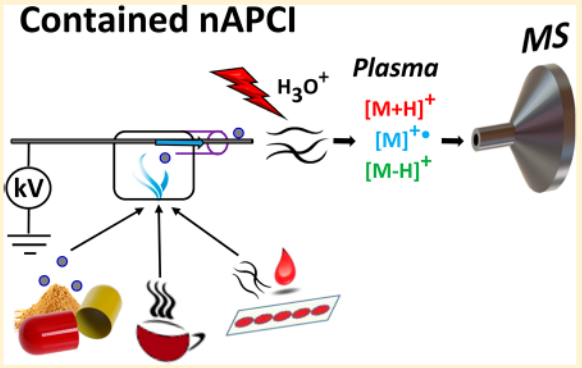

The advent of ambient ionization enabled rapid mass spectrometric analysis of complex mixtures without pretreatment.[1−7] This capability was made possible through various desorption processes that preferentially extracted and transferred the analyte of interest (not the whole multiphase sample) to the mass spectrometer. This feature of ambient ionization is attractive because the experiments are performed outside of the vacuum environment of the mass spectrometer, allowing direct access to the sample during analysis. In the current study, we show that ambient ionization of analytes having negligible vapor pressures (VP < 10^{-2} to 10^{-12} kPa) can be achieved through a novel reactive olfaction sampling process (i.e., the attraction/movement of particles caused by an electrically biased electrode that is placed close to the samples but without physical contact). This is contrary to the typical ambient ionization procedure, which rely on desorption ionization achieved via the use of high-energy-charged droplets, photons, or fast-moving gas stream of reagent ions.[8−15] We demonstrate this reactive olfaction phenomenon through the development of a new contained nano-atmospheric pressure chemical ionization (nAPCI) source.

Atmospheric pressure chemical ionization (APCI) is a popular complement to electrospray ionization (ESI). Conventional APCI experiments often use nebulizer gases whose main functions are to aid solvent evaporation through the formation of smaller liquid droplets and to serve as the source of reagent ions, in the presence of a corona discharge, which subsequently ionize the analyte via chemical ionization at atmospheric pressure. Whereas the terminal active reagent ions in APCI typically involve protonated water clusters $H^+(H_2O)_n$,[16,17] analyte energy deposition is controlled by the type of nebulizer gas used. For example, N_2 gas is observed to generate reactive and energetic reagent ions, resulting in more analyte fragmentation compared to O_2.[18] The APCI mass spectrometry (MS) methodology can be used to detect headspace vapor of volatile organic compounds,[19−21] but perhaps the strength of the method is in the delivery of less volatile analytes in the form of nebulized mist of gas stream, enabling direct coupling to liquid chromatography.[22,23] Interests in ambient ionization motivated the development of atmospheric-pressure solids analysis probe (ASAP)[24,25] and desorption atmospheric pressure chemical ionization (DAPCI) methods.[26,27] In ASAP, heated N_2 gas is used to vaporize a solid sample present in a melting glass capillary; the analyte vapor is then transferred to the ion source region where it is ionized by the corona discharge. In DAPCI, the flow direction of the nebulizer gas (He or N_2) is coaxial with the discharge needle so analyte desorption occurs using the resultant APCI reagent ions, which are carried in the gas stream. Here, the planar surface containing the sample may be heated to facilitate the desorption process.

The contained nAPCI experiment presented in this study enables the analysis of both volatile and nonvolatile organic compounds without the use of nebulizer gas or the application of heat. This discovery was inspired by our ongoing interest in contained ion sources (i.e., ionization processes in which the ionizing particles, modifying reagents, and the nebulizer gas are all constrained/contained in a single device)[28,29] as they

Received: February 15, 2019
Accepted: April 28, 2019
Published: April 28, 2019

DOI: 10.1021/acs.analchem.9b00857
Anal. Chem. XXXX, XXX, XXX−XXX

provide a means to perform ionization and ionic reactions in a single step. We discovered that headspace vapors of solids and liquids are effectively ionized when brought or "contained" in close proximity to a corona discharge generated by the application of 6 kV direct current (DC) voltage to a silver electrode (field strength is 10^6 V/m). Ionization of gas-phase analytes occurs via chemical ionization at atmospheric pressure and ambient temperature. The main distinguishing features of this new contained nAPCI ion source are 6-fold: (1) Sample introduction/conversion from the condensed phase into vapor phase is achieved either by monitoring the headspace area above the sample[30] or via an electrostatic charge induction mechanism, the combination of which is referred to here as "reactive olfaction" to mimic sniffing processes found in dogs and other animals, which also occurs through a noncontact mechanism.[31,32] (2) The contained nAPCI MS platform is able to analyze complex mixtures with high sensitivity without sample preparation at a sample consumption rate less than nmol/min. (3) The smaller sample flow rates in turn minimize carryover and contamination issues while the containment capabilities of our experimental setup allow concentration of analyte vapor into a small space for sensitive detection and quantification. (4) The containment of the condensed-phase sample in a separate vial makes our method minimally destructive, providing a convenient way to reanalyze the sample by other analytical techniques. (5) It is capable of ionizing a broad range of analytes (solids, liquids, and gases) with different physicochemical properties including volatility, polarity, and basicity/acidity, all in the positive-ion mode. (6) The proposed ion source is versatile in its ability to facilitate both gas-phase and surface-assisted ionization, yielding different ion types such as $M^{+\bullet}$, $(M + H)^+$, $(M - H)^+$, and $[M + (3H)]^+$ species, which make it possible to detect diverse groups of chemical compounds. Collectively, these features enabled direct analysis of solid particles (powder), raw biofluids, fragrances, and beverages, without prior analyte extraction or concentration. We expect such capabilities to benefit many fields including counterfeit detection, biomedical research, forensic applications, and food chemistry.

EXPERIMENTAL SECTION

Development of Contained nAPCI Source. In its fully operational form, the contained nAPCI apparatus consists of an Ag electrode inserted into disposable glass capillary. This assembly is in turn inserted into a PTFE container (2 mL) which has a stationary screw cap on the bottom (9 mm thread and 6 mm center hole) to introduce a screw top glass vial that contains the sample and from which the headspace vapor and/or particles of the analyte is supplied via the glass capillary to the corona discharge (red thunder symbol; Figure 1). A DC voltage (4–6 kV) applied to the Ag electrode enables the production of corona discharge for direct interaction and ionization of analyte vapor/particles under ambient conditions. The PTFE container itself embodies a valve on the side; the analysis of samples with negligible vapor pressures (VP) was achieved simply by opening this valve, which increases the access/flow rate of analyte's vapor/particles from the sample to the tip of the Ag electrode for plasma ionization. Note: the condensed-phase sample (solid or liquid) is placed in the glass vial.

Conventional APCI Experiments. A homemade APCI ion source was created to compare its performance to that of the proposed contained-nAPCI experimental setup. This

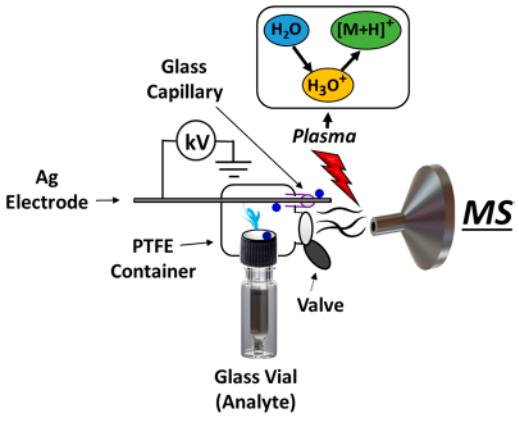

Figure 1. Experimental setup for contained nAPCI MS method. Corona discharge is generated at the tip of the Ag electrode when DC voltage >4 kV is applied. The presence of the potential also causes reactive olfaction, which increases the amount of analytes in the vapor for samples with negligible vapor pressure. The PTFE container helps to concentrate the vapor-phase molecules/particles into a small space and the glass capillary collimates the vapor toward the plasma (red thunder). When activated, the valve on the side of the PTFE container increases vapor flow rate by reducing the saturation of air above the sample.

conventional homemade APCI source consisted of a stainless steel APCI needle positioned in front of an electrospray source. A heated tube (5 mm i.d., 50 mm in length) was inserted between the ESI emitter and the APCI needle to mimic the commercial source where gas-phase species (not droplets) are exposed to the corona discharge. A DC voltage of 4 kV was supplied to the APCI needle.

Mass Spectrometry and Other Measurements. Experiments were conducted by Velos Pro LTQ and LTQ Orbitrap (for high-resolution data) mass spectrometers with Xcalibur 2.2 SP1 software (Thermo Fisher Scientific, San Jose, CA, USA). Applied parameters were as follows: DC voltage for corona discharge (6 kV for Velos Pro LTQ and 4 kV for LTQ Orbitrap); 400 °C transfer capillary temperature; 5 mm distance from ion source to MS analyzer inlet; 100 ms ion injection time; 3 microscans; 30 s time for spectra recording. S-lens (for Velos Pro LTQ) and tube lens (for LTQ Orbitrap) voltages were tuned for each analyte individually. Analyte identification was performed by Orbitrap MS and tandem MS techniques: collision-induced dissociation (CID) and higher-energy collisional dissociation (HCD). pH measurements were conducted by using a S220 pH/Ion Meter (Mettler Toledo, Schwerzenbach, Switzerland).

Chemicals, Reagents, and Samples. Acetic acid (99.7%), adipic acid (99%), anthracene (90–95%), L-ascorbic acid (99.0%), benzaldehyde (99%), benzene (99.8), carminic acid (90%), caffeine (99.0%), citral (95%), ergocalciferol (vitamin D2, 98%), β-estradiol (98%), furfural (99%), hydrocortisone (98%), methyl anthranilate (98%), palmitic acid (99%), *p*-cymene (99%), 3,5-dimethyl-1-hexyn-3-ol (Surfynol 61, 98%), ethyl myristate (97%), Girard's T reagent (99%), toluene (99.8%), 2,4,6-triphenylpyrylium tetrafluoroborate (98%), and screw top glass vial with 9 mm screw thread neck and glass vial/insert (0.5 mL) were all obtained from Sigma-Aldrich (St. Louis, USA). Benzoic acid (99.5%), 1-*n*-butyl-3-methylimidazolium di-*n*-butyl phosphate (96%), L-cysteine (99%), 1,3-dimethylimidazolium methyl sulfate (98.0%), 1-ethyl-3-methylimidazolium tetrafluoroborate

DOI: 10.1021/acs.analchem.9b00857
Anal. Chem. XXXX, XXX, XXX−XXX

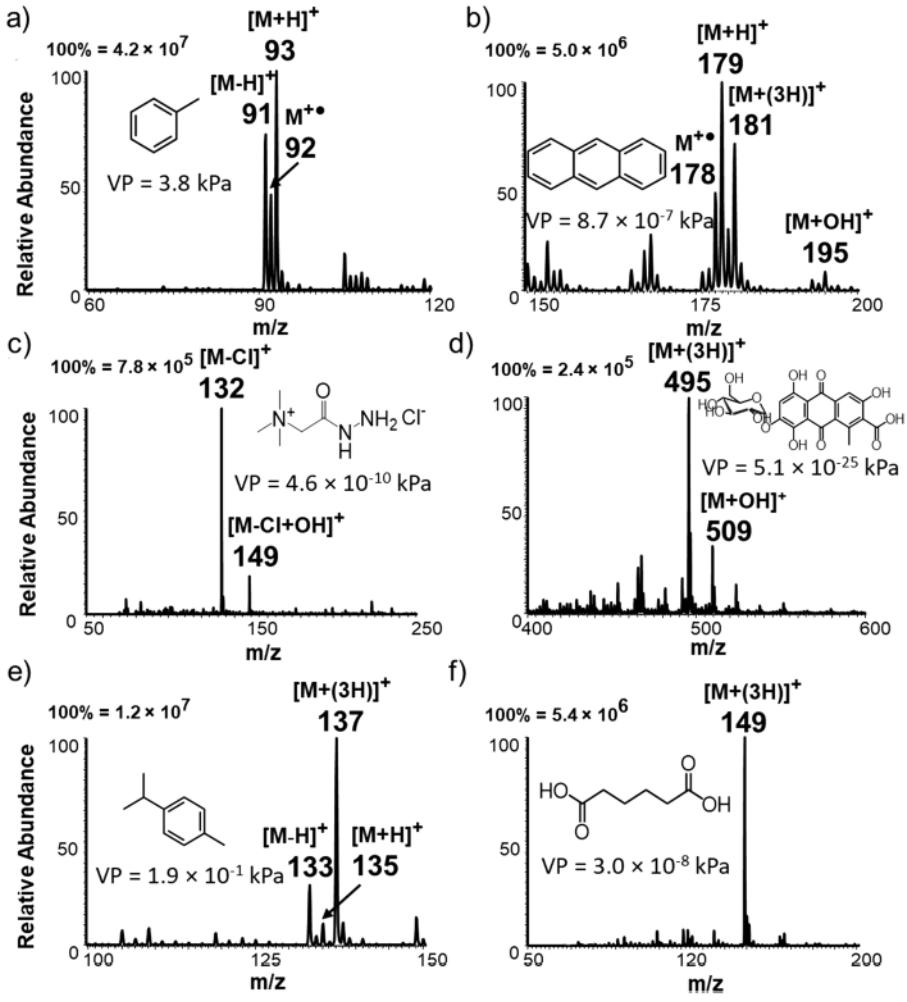

Figure 2. Contained nAPCI positive-ion mass spectra for (a) toluene, (b) anthracene, (c) Girard T reagent, (d) carminic acid, (e) *p*-cymene, and (f) adipic acid recorded using 6 kV discharge voltage.

(99%), horse serum (Gibco), L-methionine (98%), and nitric acid (15.8 M) were supplied by Fisher Scientific (Pittsburgh, PA, USA). Standard solutions of cocaine (1.0 mg/mL) were purchased from Cerilliant (Round Rock, TX, USA). Piperonal (99%) was provided by Acros Organics (Geel, Belgium). Pyrogallic acid was supplied by J.T. Baker (Phillipsburg, NJ, USA). Normal single-donor human urine was acquired from Innovative Research (Novi, MI, USA). Ground coffee Arabica (medium roast) was supplied by Gevalia (Netherlands, Amsterdam). Instant coffee Beaumont (medium roast) was bought from Aldi (Essen, Germany). Instant coffee Nescafe Clasico (dark roast) was provided by Nescafe (Vevey, Vaud, Switzerland). Cherry Coca Cola, Fanta, and Mello Yello bottled drinks were obtained from Coca Cola Company (Atlanta, GA, USA). Dolce&Gabbana Pour Femme Eau de Parfum was supplied from the manufacturer (Milan, Italy) and Touch of Spring Eau de Toilette Spray was purchased from Lacoste (Troyes, France). Old Spice (Pure Sport) body spray was provided by Procter & Gamble (Cincinnati, OH, USA). Silver electrode (0.2 mm diameter) was acquired from Warner Instruments (Hamden, CT, USA). Borosilicate capillaries (i.d. 1.17 mm) were supplied by Sutter Industries (Novato, CA, USA). Water (18.2 MΩ) was used for all water-based solutions (Milli-Q water purification system, Millipore, Billerica, MA, USA). The rest of the ∼60 compounds and samples tested in this work are listed in the Supporting Information.

RESULTS AND DISCUSSION

Optimization and Ion Type Characterization. The contained nAPCI source was first optimized using volatile toluene analyte (VP = 3.8 kPa) and a representative positive-ion-contained nAPCI mass spectrum is shown in Figure 2a. This spectrum was recorded after applying optimized 6 kV of DC voltage to the Ag electrode, which registered three ionic species: hydride elimination to yield $[M - H]^+$ ions at m/z 91, molecular ion ($M^{+\bullet}$) at m/z 92, and protonated $[M + H]^+$ species at m/z 93. Similar ion types were also derived from the headspace vapor analysis of anthracene (VP = 8.7×10^{-7} kPa;

Scheme 1. Possible Mechanism for Surface-Assisted Hydrogenation of C═O and C═C Bonds[a]

$$M_{(ads)} \xrightarrow[H^+]{e^-} MH_{(ads)} \xrightarrow[H^+]{e^-} MH_{2(ads)} \longrightarrow MH_{2\ (gas)}$$

[a]Analyte (M) is adsorbed (ads) on metal electrode during corona discharge, which facilitates its reduction via two sequential reactions with protons and electrons. Reaction is followed by desorption of products into the gas phase.

DOI: 10.1021/acs.analchem.9b00857
Anal. Chem. XXXX, XXX, XXX−XXX

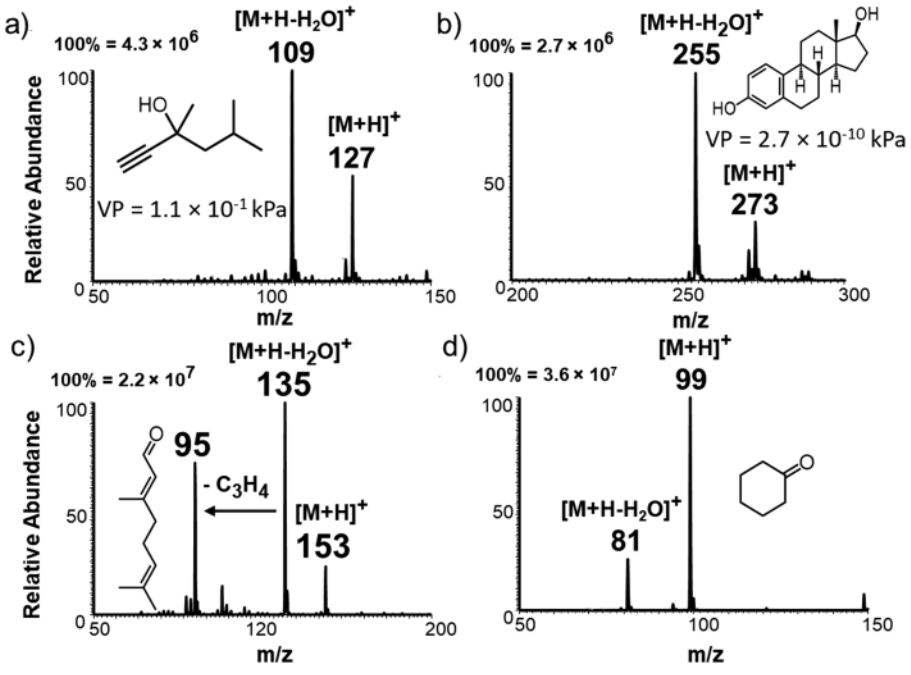

Figure 3. Contained nAPCI MS analysis of the following: (a) Surfynol 61, (b) β-estradiol, (c) citral, and (d) cyclohexanone. Peak at m/z 95 in (c) is assigned to a loss of cyclopropene (C_3H_4) from the ion at m/z 135.

Figure 2b) and other hydrocarbons such as cyclohexane, benzene, and naphthalene (Table S1, Supporting Information; all compounds were analyzed at 6 kV discharge voltage unless otherwise stated). These results are comparable to those recorded from conventional APCI and its related experiments,[33] except that no pneumatic assistance was employed in the current vapor-phase ionization process. Under this condition, Girard reagent T (VP = 4.6×10^{-10} kPa), a nonvolatile organic salt having quaternary ammonium species, was sensitively detected at m/z 132 (the valve open) with no heat supplied to the sample container (Figure 2c). The elimination of heat and reagent gases provide simplicity in experimental setup and speed in chemical analysis compared to the corresponding desorption-based ionization methods.

The limit of the contained nAPCI ion source was further tested through the analysis of carminic acid (MW 492 Da), which has a negligible vapor pressure of 5.1×10^{-25} kPa (low/unknown VPs were estimated).[34] Whereas volatile and semivolatile analytes produced ion types similar to those observed in other APCI experiments, a unique ionic species $[M + (3H)]^+$ was abundantly detected at m/z 495 (Figure 2d) from the untreated solid (powder) carminic sample. The production of this ion type in our contained nAPCI source was also observed for anthracene, *p*-cymene, and adipic acid (Figure 2b,e,f). Similar levels of $[M + (3H)]^+$ ion signal were observed from other metals (Pt and Fe, 0.25 mm i.d.) and nonmetal (graphite, 0.3 mm i.d.) electrodes (Figure S1) as well as from Ag electrodes of different surface areas (see Figure S2 for details). This suggests that the process, which appears to be the addition of two hydrogen atoms across C═C and C═O bonds, is field-induced. In other words, the main role of the electrode might involve the uncatalytic adsorption of analyte, increasing its residence time for effective reaction with electrons and protons from the plasma. Similar hydrogenation reaction was reported by Cooks' group when naphthalene and other aromatic hydrocarbon and N-heterocyclic compounds were exposed to low-temperature plasma.[35] Molecular ions $(M + 2H)^{\bullet+}$ of the hydrogenation products were detected, which was attributed to surface-assisted reactions involving adsorbed electrons and protons from the plasma. We believe protonated species $H^+(M + 2H)$ of similar reaction products are observed in our contained-nAPCI source.

The presence of this $[M + (3H)]^+$ ion clearly reveals that the mechanism of ion production in the contained nAPCI ion source is not just due to gas-phase chemical ionization as is typically the case in regular APCI. Instead, reactions occurring at the electrode surface may contribute substantially. Because the resultant gas-phase ions are generated from proximal condensed-phase samples with no physical contact, it is reasonable to propose that the first step in the surface-assisted ionization process must involve the attraction of particles from the proximal solid (powder) sample to the electrode via electrostatic charge induction (see Video S1, discussed in detail in the Supporting Information). The process leading to the generation of $[M + (3H)]^+$ ion from solid carminic acid is depicted in Scheme 1, where electrostatic charge induction causes the attraction of analyte particles to the electrode. The adsorbed analyte particles (M_{ads}) interact with protons and electrons from the corona discharge, in two sequential events. The hydrogenation reaction then occurs on the surface of the adsorbed analyte particles. The reaction product (MH_2, Scheme 1) is ionized through field-induced protonation reactions or via APCI mechanism involving the desorbed gas-phase $(MH_2)_{gas}$ species. Further experiments with D_2O vapor involving *p*-cymene and carminic acid analytes registered the presence of abundant $[M + 2D]^+$ and $[M + 3D]^+$ species when the D_2O vapor was brought in close proximity to the Ag electrode where the corona discharge is created (Figure S3). This result confirms that the protons involved in the observed hydrogenation reaction are derived from an external source (e.g., from the plasma) and not from the analytes themselves as illustrated in Scheme 1.

Aside from the analysis of proximal nonvolatile solid (powder) samples, the contained nAPCI source enabled the

DOI: 10.1021/acs.analchem.9b00857
Anal. Chem. XXXX, XXX, XXX−XXX

Table 1. Chemical and Physical Properties of Different Types of Compounds with MS^2 Data for nAPCI Analysis[a]

#	Compound	Structure	MW (Da)	VP (kPa, 25°C)	Observed Ion(s)	MS^2 Transition(s) (CID)
1	Vitamin D2†*	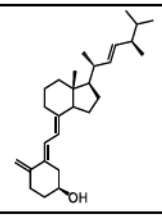	397	8.5×10^{-11}	$M^{+\bullet}$	397 → 379, 369, 351, 327, 271
					$[M+H]^+$	398 → 380, 370, 352, 328, 272
					$[M-H_2O]^+$	379 → 323, 309, 295, 283, 253, 199
2	Hydrocortisone†*	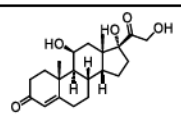	362	1.6×10^{-14}	$[M+H]^+$	363 → 345, 327, 309, 297, 267, 121
					$[M-H]^+$	361 → 343, 325, 297, 279, 121
3	Ethyl myristate	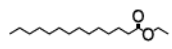	256	2.7×10^{-4}	$[M+H]^+$	257 → 229, 191
					$[M+H-CO]^+$	229 → 201, 159, 131, 117, 103, 89
4	L-Ascorbic acid†*	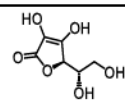	176	2.4×10^{-11}	$[M+H]^+$	177 → 159, 149, 135, 121, 107, 95
					$[M-H]^+$	175 → 157, 147, 133, 119, 105
5	Citral*	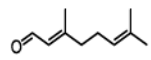	152	1.2×10^{-2}	$[M+H-H_2O]^+$	135 → 119, 107, 93, 79
					$[M+H-H_2O-C_3H_4]^+$	95 → 67, 55, 41 (HCD)
					$[M+H]^+$	153 → 135, 109, 95, 81
6	Piperonal	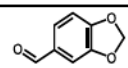	150	1.3×10^{-3}	$[M+H]^+$	151 → 123, 93
7	L-Methionine†*	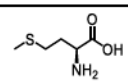	149	7.8×10^{-8}	$[M+H]^+$	150 → 133, 104, 87, 74 (HCD)
					$[M+H-OH]^+$	133 → 105, 87, 75
8	Pyrogallic acid		126	6.4×10^{-5}	$[M+H]^+$	127 → 109, 99, 85
					$[M-H]^+$	125 → 107, 97
9	L-Cysteine†*	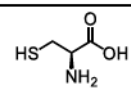	121	9.0×10^{-8}	$[M+H]^+$	122 → 105, 94, 76

[a]The dagger symbol (†) represents data that was analyzed with an open valve to increase ion signal intensity. The asterisk (*) represents the vapor pressure (VP) determined by Estimation Program Interface (EPI) Suite 4.1 software.[19] Abbreviations: HCD, high-energy collision dissociation. CID, collision-induced dissociation.

ionization of ionic liquids (1-ethyl-3-methylimidazolium tetrafluoroborate and 1,3-dimethylimidazolium methyl sulfate), which are also known to have negligible vapor pressures.[36−39] For 1-ethyl-3-methyl-1,3-imidazolium tetrafluoroborate, we observed abundant fragment ion signal in positive mode at m/z 83 and 99 that corresponded to the loss of ethylene ($CH_2{=}CH_2$, MW 28 Da) from the cation (Cat) and [Cat + O]$^+$ counterparts of the ionic liquid, respectively (Figure S4a). Each fragment ion was characterized by tandem MS (see Figure S4b−d for details). The anion counterpart of 1,3-dimethylimidazolium methyl sulfate was detected at m/z 111 in the negative ion mode (Figure S5). This and other results discussed above indicate the contained nAPCI source as being reactive. In this regard, we observed dehydrated species [M + H − H_2O]$^+$ from ketones, aldehydes, and alcohols (Figure 3) as well as the generation of [M + OH]$^+$ ions[40,41] (e.g., anthracene (Figure 2b), iodobenzene, and aniline Figure S6). The identity of analytes were confirmed through tandem MS experiments using collision-induced dissociation (select compounds provided in Table 1). A list of all 80 compounds tested and their corresponding ion types are also provided in Table S1. Note that the contained nAPCI setup is not limited to the 0.5 mL sample size used here. For example, high ion intensities were recorded from only 1 μL of 1-*n*-butyl-3-methylimidazolium di-*n*-butyl phosphate ionic liquid (Figure S7), which registered fragment ions at m/z 83 and 99 derived from the elimination of 1-butene from the cation (Cat) and [Cat + O]$^+$,[40−42] respectively.

Electrostatic Charge Induction and Reactive Olfaction. The ion types (e.g., [M + (3H)]$^+$) and the high sensitivity observed in the contained nAPCI experiment suggest that the total analyte vapor concentration results from the combined effects of (natural) analyte vapor pressure and electrostatic charging[43] of the proximal condensed-phase sample. In electrostatic charging, the applied DC voltage is expected to induce the separation of partial positive (δ+) and negative (δ−) charges. Charges of the same polarities accumulate in close proximity, in response to the applied voltage, which leads to the instantaneous liberation/movement of particles as a result of Coulombic repulsion (Video S1). The

DOI: 10.1021/acs.analchem.9b00857
Anal. Chem. XXXX, XXX, XXX−XXX

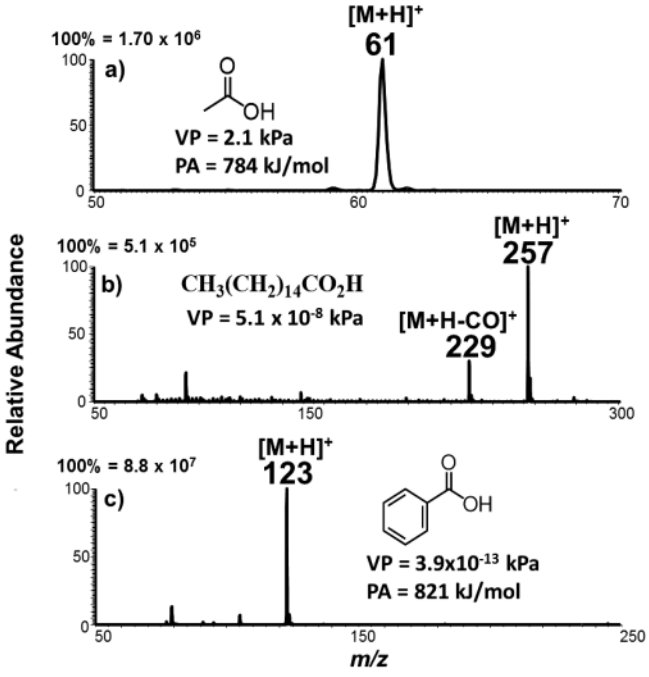

Figure 4. Positive-ion mass spectra obtained after contained nAPCI MS analysis of (a) acetic acid, (b) palmitic acid, and (c) benzoic acid (with the open valve).

resultant effect (i.e., particle movement) is similar to that observed in electroscope experiments in which the two metal leaves separate (move apart) as a result of charge induction. Another well-known example is found in field charging (or electrostatic precipitation) where aerosols/particles are caused to move in corona discharge.[44−47] We suggest to call this phenomenon and its application to MS analysis as reactive olfaction. We have observed the number of electrostatically liberated vapor-phase particles to be directly proportional to applied voltage (Figure S8) and distance between the Ag electrode and the sample (Figure S9), an effect that is consistent with Coulomb's law ($F_e \sim (q_1q_2)/r^2$), where q represents charges on the electrode and a surface particle and r is the distance between the electrode and the particle. Therefore, the geometry of contained nAPCI apparatus was optimized in terms of distance between the electrode and analyte (5 mm) to maximize the ion signal (Figure S9). The distance between the electrode and MS was optimized as well (5 mm; Figure S10) to improve signal intensity and to avoid sparking. Moreover, to increase the amount of analytes in vapor phase for compounds with negligible vapor pressure (e.g., carminic acid, hydrocortisone, and vitamin D2), the discharge voltage was temporally increased (<2 s) from the typical 6 to 8 kV (i.e., a step voltage was used). This enabled effective MS analysis at 6 kV source voltage without heating or the application of a nebulizing gas. Further experiments revealed that analyte desorption is temperature-independent as demonstrated for acethydrazide trimethylammonium cation detection at MS inlet capillary temperature of 45 °C (Figure S11) and the collection of visible dye particle at ambient temperatures (Figure S8 and Video S1). For carminic acid, signal-to-noise ratio (SNR) of the $[M + (3H)]^+$ ion increased with inlet capillary temperature (Figure S12); we ascribe this effect to a more effective declustering process at higher temperatures. Note that no ion signal is observed from carminic acid without applying discharge voltage, and inlet

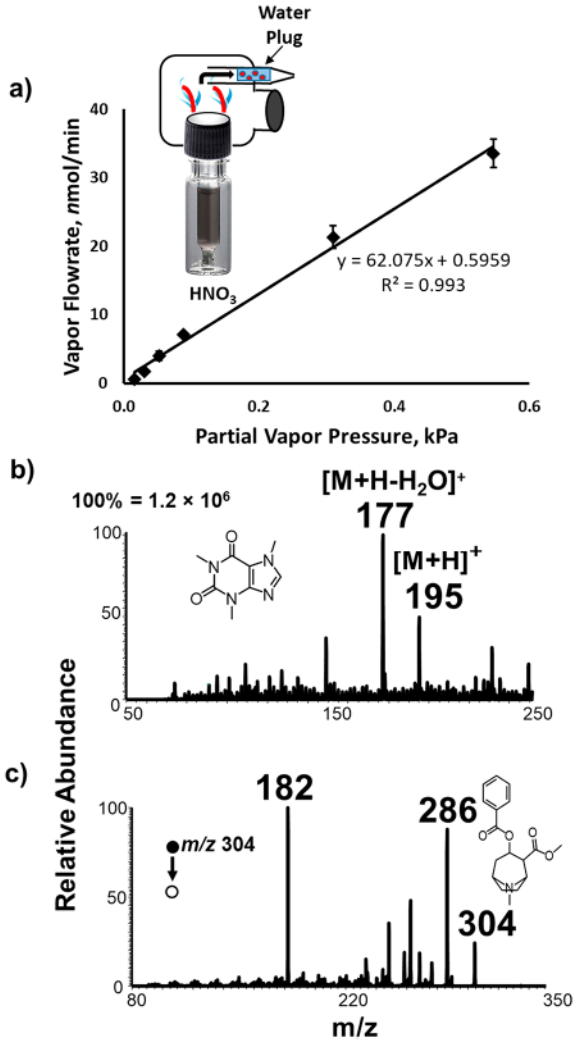

Figure 5. (a) Headspace vapor flow rate determination using HNO_3 vapor in contained nAPCI at 0 kV. Error bars indicate three-replicate analysis. (b) 200 pg/mL caffeine (VP 1.2×10^{-7} kPa) in urine and (c) MS/MS product ion spectrum of 100 ng/mL cocaine (VP 2.5×10^{-8} kPa) in serum.

ionization (direct deposition of sample at the MS inlet)[48] at 400 °C also failed to yield detectable ion signal (Figure S13), all confirming the effect of corona discharge on desorption and subsequent ionization of nonvolatile molecules like carminic acid.

The ability to electrostatically desorb/adsorb and initiate chemical reaction at the surface of discharge electrode has not been reported for any type of APCI experiment; this is presumably because the routine use of nebulizer gas in APCI experiments reduces the residence time of analyte at the electrode surface and hence there is less chance for surface-assisted chemical reactions. To investigate this possibility, we compared the performance of contained nAPCI to the conventional APCI experimental setup for the analysis of carminic acid. No signal due to $(M + 3H)^+$ ions was detected at lower concentrations of carminic acid (<1 μg/mL) when analyzed by the conventional APCI source. We observed $(M + 3H)^+$ ion signal when the concentration of carminic acid was increased to 1000 μg/mL (see Figure S14 for details). Further experiments indicated that this ion signal is actually due to surface reactions at the discharge needle. For example, at such

DOI: 10.1021/acs.analchem.9b00857
Anal. Chem. XXXX, XXX, XXX−XXX

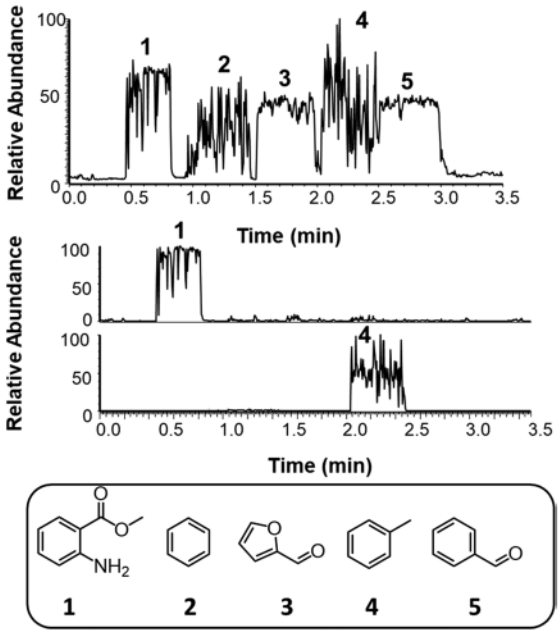

Figure 6. (a) Total ion chromatogram resulting from sequential and real-time analysis of (1) methyl anthranilate, (2) benzene, (3) furfural, (4) toluene, and (5) benzaldehyde. (b) Extracted ion chromatograms at m/z 152 (protonated compound 1) and m/z 193 (protonated compound 4) showing minimal carryover issues after removal from the source.

high concentrations, the discharge needle was seen covered with carminic acid (Figure S14c). Ion signal persisted even after terminating analyte supply from the ESI source, indicating that the observed $(M + 3H)^+$ ions originated from residues of carminic acid coated on the needle. This supports our initial proposal that surface-assisted reactions are responsible for the generation of $(M + 3H)^+$ ions in the contained-nAPCI source. Ion intensity dropped significantly when N_2 (120 psi) was used (Figure S14d), confirming the observed reaction is not a gas-phase process. No ion signal due to carminic acid was detected from the electrospray process alone, without supplying DC voltage to the discharge needle. It is important to note that using 1000 μg/mL of carminic acid solution on the conventional APCI setup to observe this surface reaction can result in a significant instrument contamination. In contrast, although the bulk solid powder of carminic acid is analyzed in our proposed contained nAPCI source, we do not observe substantial issues with contaminations because of the occurrence of the reactive olfaction phenomenon and the containment features of the ion source.

Investigating Chemical Ionization in the Contained nAPCI Source. Another interesting feature of the contained nAPCI ion source is that it predominantly produces positive ions. Figure 4 illustrates this phenomenon in which protonation occurred for organic acids like acetic acid (VP = 2.07 kPa; proton affinity (PA) = 784 kJ/mol; ionization energy (IE) = 10.65 eV). This suggests that the chemical ionization process might not involve large protonated water clusters as is typically the case in conventional APCI where high flow rates of solvents are used.[47] Note: PA of $H^+(H_2O)_n$ cluster is 878.6 and 900.0 kJ/mol for n = 2 and 3,[49] respectively, both of which cannot protonate acetic acid. This leaves us to conclude that the protonated ions observed in contained nAPCI MS are formed either by field-induced proton-transfer reaction ($M^{\bullet+}_{(surf)} + H_2O \rightarrow [M + H]^+ + HO^\bullet$) or by chemical ionization via reaction with hydronium ions (H_3O^+). Takayama and co-worker[50,51] have studied positive ion evolution in corona discharge at atmospheric pressure (in the absence of external solvents) and found that the terminal ions are H_3O^+ and $H^+(H_2O)_2$, which is consistent with the current results (Figure S15). We further investigated the influence of other factors (PA, IE, and VP) on the production and absolute intensity of the positive ions ($[M - H]^+$, $M^{+\bullet}$, $[M + H]^+$) observed in the contained nAPCI source (Figure S16a–c). No particular trend was observed except that the analyte with highest proton affinity dominated the spectrum for mixture samples. For hydrocarbon analytes, both $M^{+\bullet}$ and $[M - H]^+$ species were often observed together.[52,53]

Quantification and Direct Biofluid Analysis. As already shown, vapor pressure is not a limiting factor in contained nAPCI MS. Instead, the strength of the derived ion signal is found dependent on amount as well as vapor pressure of the sample. On the basis of gas law, the number of moles in headspace vapor is directly proportional to vapor pressure if volume and temperature are held constant. We determined this to be true in our contained nAPCI experiment using HNO_3 vapor. Here, different HNO_3 solutions were prepared at varying concentrations (40–70%), each with known vapor pressure.[54] Headspace vapor from each of the prepared HNO_3 solutions was seeded into 10 μL of water plug contained in a removable pulled glass capillary (insert, Figure 5a). After 1 h of vapor seeding, the resultant solution in which the HNO_3 vapor has been collected was diluted into 2 mL of water and the pH measured. Obtained pH values were converted into hydrogen ion concentrations, yielding headspace vapor flow rates in the nmol/min range (0.58–34 nmol/min). This flow rate represents a minimum in a typical experiment where DC voltage is applied and the reactive olfaction phenomenon is in operation. The determined vapor flow rates varied linearly with known partial pressures of HNO_3 solutions (Figure 5a) and RSD for each determination was less than 10%. As such, a calibration curve was successfully constructed for acetone, an important metabolism marker, when spiked in raw urine (Figure S17); contained nAPCI ion signal increased linearly (R^2 = 0.97) with acetone concentration, and a good limit of quantification (200 pg/mL) was observed (normal levels of urinal acetone for healthy individuals is in the range 0.2–3.9 μg/mL).[55] Similar concentration-dependent analysis was achieved for pyridine in roasted coffee (Figure S18), which was consistent with reported trends.[56] Figure 5b,c shows representative contained nAPCI mass spectra obtained from (i) direct analysis of 200 pg/mL caffeine (MW 194 Da) in raw urine (Figure 5b) where both $[M + H]^+$ and $[M + H - H_2O]^+$ species were detected at m/z 195 and 177, respectively, and (ii) 100 ng/mL cocaine (MW 303 Da) in a more complex serum matrix, which was analyzed in tandem MS (MS/MS) experiments (Figure 5c). Cocaine dissociated to give the characteristic fragment ion at m/z 182 upon collisional activation. Limit of detection for cocaine in human serum was detected at 1 ng/mL level. On the basis of vapor pressure alone, this limit will correspond to only 0.6 zmol of cocaine vapor (361 molecules) per mL of air inside our contained nAPCI source (see Figure S19 and other details in the Supporting Information). Assuming <1% ionization efficiency, this sensitivity cannot be explained only by the analyte's vapor pressure. We believe the electrostatic charge induction mechanism plays a significant role here to increase the number

DOI: 10.1021/acs.analchem.9b00857
Anal. Chem. XXXX, XXX, XXX–XXX

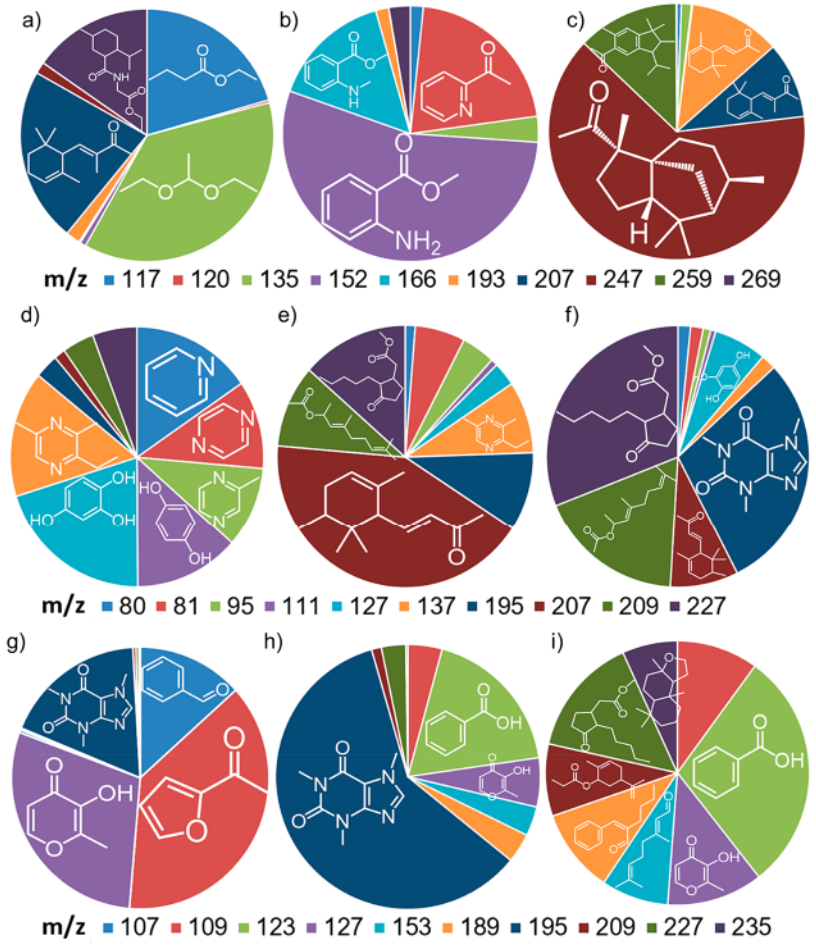

Figure 7. Comparison of headspace vapor chemical composition of perfumes (a–c), solid coffee (d–f), and carbonated drinks (g–i) achieved using positive ion contained nAPCI MS: (a) Lacoste, (b) Dolce&Gabbana, (c) Old Spice, (d) Gevalia, (e) Nescafe, (f) Beaumont, (g) Cherry Coca-Cola, (h) Mello Yello, and (i) Fanta.

of vapor-phase cocaine analyte from the nonvolatile serum sample. Carryover issues are observed to be minimal in the contained nAPCI experiment as illustrated for real-time analysis of methyl anthranilate (1), benzene (2), furfural (3), toluene (4), and benzaldehyde (5) (Figure 6a,b). These five compounds were analyzed sequentially in 30 s intervals. As exemplified in Figure 6b for 1 and 4, no trace of each compound was detected after their removal from the source (Figure S20). These results are not surprising given the modes of sample introduction (containment, not direct infusion) and analysis (noncontact sampling) by the proposed nAPCI method and the fact that only a small amount of sample (nmol) is consumed.

Direct Analysis of Perfumes and Beverages. Perhaps the most obvious application of the proposed reactive olfaction sampling method is in the direct differentiation of the chemical composition of perfumes and beverages through the detection of their abundant headspace vapors. Figure 7a–c shows results for three colognes: Lacoste, Dolce&Gabbana, and Old Spice, respectively. The structures and identities of the 25 most abundant ionic species detected from each cologne were confirmed using MS/MS experiments, and via accurate mass measurements (Table S2). Of these, the top 10 compounds are presented in Figure 7a–c, which clearly show that the three colognes can be differentiated on basis of the chemical composition of their headspace vapors, without prior extraction or preconcentration. Each major compound can be related to a distinctively known aroma or other function (e.g., UV absorption properties in Lacoste cologne), confirming their structural identification by contained nAPCI MS. For example, acetal (m/z 135; refreshing, pleasant odor) and α-isomethylionone (m/z 207; floral, woody scent) were detected as one of the most abundant compounds in Lacoste Touch of Spring, which is well-known for its fresh, floral, and sandalwood notes (Figure 7a). The orange blossom and jasmine middle notes of Dolce&Gabbana Femme perfume was also confirmed using nAPCI MS by detection of methyl anthranilate (m/z 152; orange-flower odor) and methyl *N*-methylanthranilate (m/z 166; fruity, floral scent).

The same olfaction approach was applied for the analyses of coffee (Figure 7d–f, Figure S18 and Table S3) and carbonated drinks (Figure 7g–i, Figure S21, and Table S4). Here, too, the top 26 most abundant ionic species were characterized for two types of ground coffee, two types of instant coffee, and three types of brewed coffee with different roast levels (Table S3). Whereas solid coffee showed distinct composition for volatile and nonvolatile components, brewed coffee was found to be very similar by headspace vapor chemistry. However, the abundance of pyridine was dramatically increased from light roast to dark roast coffee, a result that is in good agreement with coffee chemistry in which the alkaloid trigonelline partially degrades during roasting to produce pyridine and

DOI: 10.1021/acs.analchem.9b00857
Anal. Chem. XXXX, XXX, XXX−XXX

nicotinic acid[57] (Figure S18a). Clearly, these results suggest that the contained nAPCI technique can find use in counterfeit analysis related to the perfume and food industry, allowing analysis in less than a minute (with no need for sample preparation) after comparison to authentic samples with known fingerprints of chemical constituents.

Finally, five Coca-Cola carbonated drinks (Cherry Coca-Cola, Mello Yello, Fanta, Coca-Cola, and Sprite) were analyzed without sample preparation and no physical contact or heating. We detected different caffeine contents and unique compounds that can be related to known flavors. For example, a large amount of benzaldehyde (m/z 107; cherry flavor) was detected in Cherry Cola, which is absent in all other carbonated drinks tested (Figure 7g–i). The reactive olfaction sampling confirmed Mello Yello to be a highly caffeinated, citrus-flavored soft drink (Figure 7h). No caffeine, m/z 195, was detected in Fanta and Sprite as prescribed by Coca-Cola Company (Figure 7i and Figures S21 and S22). Maltol (m/z 127; caramellic flavor), was detected more abundantly in the cola drinks (e.g., Coca-Cola and Cherry Cola) compared to the citrus-flavored beverages (e.g., Fanta and Mello Yello). Preservatives such as benzoic acid (m/z 123) were also detected in all the tested carbonated drinks. These consistent results demonstrate that because of its high sensitivity the new contained nAPCI MS platform can provide a unique opportunity to rapidly study not only odor but also flavor chemistry using headspace vapors, which hold promise in food chemistry applications.

CONCLUSION

In summary, we have demonstrated a new ambient ionization method (contained nAPCI) to generate gas-phase ions from analytes with negligible vapor pressures (as low as 10^{-25} kPa). The predominant production of different positive ions is advantageous because it adds a new dimension to the array of mass spectrometric methods available for structural studies. The ultrahigh sensitivity of the method enabled the detection of nonvolatile analytes present in complex mixtures (including biofluids) through the reactive olfaction mechanism that limit matrix effect by offering low sampling rates and the containment feature of the ion source that allow preconcentration effects. The simplicity of the reactive olfaction process occurring without heat and nebulizing gas as well as in the absence of sample preparation, and the possibility of sample reanalysis by other methods due to minimal sample consumption/destruction in the contained nAPCI give these findings potential to have promising analytical applications. These results, including the ability to generate different ion types, point to the unexpected possibility that many compounds irrespective of their states of matter, polarity, volatility, and basicity/acidity can be rapidly analyzed by this simple contained nAPCI MS platform rather than switching between different ion sources.

ASSOCIATED CONTENT

Supporting Information

The Supporting Information is available free of charge on the ACS Publications website at DOI: 10.1021/acs.analchem.9b00857.

Additional material including materials, instrumentation, full experimental details and additional figures and tables (PDF)

Video of reactive olfaction involving the attraction/liberation of particles from the proximal solid (powder) sample to the electrode via electrostatic charge induction, without a physical contact (ZIP)

AUTHOR INFORMATION

Corresponding Author

*E-mail: badu-tawiah.1@osu.edu. Tel.: 614-292-4276. Fax: (614) 292-1685.

ORCID

Abraham K. Badu-Tawiah: 0000-0001-8642-3431

Notes

The authors declare no competing financial interest.

ACKNOWLEDGMENTS

This work was supported by the Ohio State University Start-up funds and NSF through the NSF Center for Aerosol Impacts on Chemistry of the Environment (CAICE), CHE-1801971. A.K.B.-T., T.S., and Q.W. thank the U.S. Department of Energy, Office of Science, Office of Basic Energy Sciences, Condensed Phase and Interfacial Molecular Science, under award number DE-SC0016044, for funding.

REFERENCES

(1) Takáts, Z.; Wiseman, J. M.; Gologan, B.; Cooks, R. G. *Science* **2004**, *306*, 471–473.
(2) Cody, R. B.; Laramée, J. A.; Durst, H. D. *Anal. Chem.* **2005**, *77*, 2297–2302.
(3) Wang, H.; Liu, J.; Cooks, R. G.; Ouyang, Z. *Angew. Chem., Int. Ed.* **2010**, *49*, 877–880.
(4) Laskin, J.; Heath, B. S.; Roach, P. J.; Cazares, L.; Semmes, O. J. *Anal. Chem.* **2012**, *84*, 141–148.
(5) Andrade, F. J.; Shelley, J. T.; Wetzel, W. C.; Webb, M. R.; Gamez, G.; Ray, S. J.; Hieftje, G. M. *Anal. Chem.* **2008**, *80*, 2654–2663.
(6) Monge, M. E.; Harris, G. A.; Dwivedi, P.; Fernández, F. M. *Chem. Rev.* **2013**, *113*, 2269–2308.
(7) Black, C.; Chevallier, O. P.; Elliott, C. T. *TrAC, Trends Anal. Chem.* **2016**, *82*, 268–278.
(8) Venter, A.; Sojka, P. E.; Cooks, R. G. *Anal. Chem.* **2006**, *78*, 8549–8555.
(9) Peng, I. X.; Ogorzalek Loo, R. R.; Margalith, E.; Little, M. W.; Loo, J. A. *Analyst* **2010**, *135*, 767–772.
(10) Nemes, P.; Vertes, A. *Anal. Chem.* **2007**, *79*, 8098–8106.
(11) Sampson, J. S.; Hawkridge, A. M.; Muddiman, D. C. *J. Am. Soc. Mass Spectrom.* **2006**, *17*, 1712–1716.
(12) Gross, J. H. *Anal. Bioanal. Chem.* **2014**, *406*, 63–80.
(13) Spencer, S. E.; Tyler, C. A.; Tolocka, M. P.; Glish, G. L. *Anal. Chem.* **2015**, *87*, 2249–2254.
(14) Andrade, F. J.; Shelley, J. T.; Wetzel, W. C.; Webb, M. R.; Gamez, G.; Ray, S. J.; Hieftje, G. M. *Anal. Chem.* **2008**, *80*, 2646–2653.
(15) Beckey, H. D. In *Principles of Field Ionization and Field Desorption in Mass Spectrometry*: Pergamon: Oxford, 1977; p 354.
(16) Ding, X.; Duan, Y. *Mass Spectrom. Rev.* **2015**, *34*, 449–473.
(17) Smoluch, M.; Mielczarek, P.; Silberring, J. *Mass Spectrom. Rev.* **2016**, *35*, 22–34.
(18) Jin, C.; Viidanoja, J.; Li, M.; Zhang, Y.; Ikonen, E.; Root, A.; Romanczyk, M.; Manheim, J.; Dziekonski, E.; Kenttämaa, H. I. *Anal. Chem.* **2016**, *88*, 10592–10598.
(19) Mulligan, C. C.; Justes, D. R.; Noll, R. J.; Sanders, N. L.; Laughlin, B. C.; Cooks, R. G. *Analyst* **2006**, *131*, 556–567.
(20) Badjagbo, K.; Picard, P.; Moore, S.; Sauvé, S. *J. Am. Soc. Mass Spectrom.* **2009**, *20*, 829–836.

DOI: 10.1021/acs.analchem.9b00857
Anal. Chem. XXXX, XXX, XXX–XXX

(21) Huang, G.; Gao, L.; Duncan, J.; Harper, J. D.; Sanders, N. L.; Ouyang, Z.; Cooks, R. G. *J. Am. Soc. Mass Spectrom.* **2010**, *21*, 132−135.
(22) Thomson, B. A. *J. Am. Soc. Mass Spectrom.* **1998**, *9*, 187−193.
(23) Cirigliano, A. M.; Rodriguez, M. A.; Gagliano, M. L.; Bertinetti, B. V.; Godeas, A. M.; Cabrera, G. M. *J. Chromatogr. A* **2016**, *1439*, 97−111.
(24) McEwen, C. N.; McKay, R. G.; Larsen, B. S. *Anal. Chem.* **2005**, *77*, 7826−7831.
(25) Gaiffe, G.; Cole, R. B.; Lacpatia, S.; Bridoux, M. C. *Anal. Chem.* **2018**, *90*, 6035−6042.
(26) Takats, Z.; Cotte-Rodriguez, I.; Talaty, N.; Chen, H. W.; Cooks, R. G. *Chem. Commun.* **2005**, *0*, 1950−1952.
(27) Chen, H.; Zheng, J.; Zhang, X.; Luo, M.; Wang, Z.; Qiao, X. *J. Mass Spectrom.* **2007**, *42*, 1045−1056.
(28) Kulyk, D. S.; Miller, C. F.; Badu-Tawiah, A. K. *Anal. Chem.* **2015**, *87*, 10988−10994.
(29) Miller, C. F.; Kulyk, D. S.; Kim, J. W.; Badu-Tawiah, A. K. *Analyst* **2017**, *142*, 2152−2160.
(30) Giannoukos, S.; Brkić, B.; Taylor, S.; Marshall, A.; Verbeck, G. F. *Chem. Rev.* **2016**, *116*, 8146−8172.
(31) Craven, B. A.; Paterson, E. G.; Settles, G. S. *J. R. Soc., Interface* **2010**, *7*, 933−943.
(32) Staymates, M. E.; MacCrehan, W. A.; Staymates, J. L.; Kunz, R. R.; Mendum, T.; Ong, T.-H.; Geurtsen, G.; Gillen, G. J.; Craven, B. A. *Sci. Rep.* **2016**, *6*, 36876.
(33) Jjunju, F. P. M.; Maher, S.; Li, A.; Badu-Tawiah, A. K.; Taylor, S.; Cooks, R. G. *J. Am. Soc. Mass Spectrom.* **2015**, *26*, 271−280.
(34) Software for estimating vapor pressures (EPI Suite - Estimation Program Interface v4.11) was provided by United States Environmental Protection Agency. https://www.epa.gov/tsca-screening-tools/download-epi-suitetm-estimation-program-interface-v411. Accessed June 22, 2018.
(35) Na, N.; Xia, Y.; Zhu, Z.; Zhang, X.; Cooks, R. G. *Angew. Chem., Int. Ed.* **2009**, *48*, 2017−2019.
(36) Dupont, J.; Spencer, J. *Angew. Chem.* **2004**, *116*, 5408−5409.
(37) Dupont, J.; Spencer, J. *Angew. Chem., Int. Ed.* **2004**, *43*, 5296−5297.
(38) Welton, T. *Chem. Rev.* **1999**, *99*, 2071−2084.
(39) Chen, H.; Ouyang, Z.; Cooks, R. G. *Angew. Chem.* **2006**, *118*, 3738−3742.
(40) Wolf, J.-C.; Gyr, L.; Mirabelli, M. F.; Schaer, M.; Siegenthaler, P.; Zenobi, R. *J. Am. Soc. Mass Spectrom.* **2016**, *27*, 1468−1475.
(41) Wu, C.; Qian, K.; Nefliu, M.; Cooks, R. G. *J. Am. Soc. Mass Spectrom.* **2010**, *21*, 261−267.
(42) Ayrton, S. T.; Jones, R.; Douce, D. S.; Morris, M. R.; Cooks, R. G. *Angew. Chem., Int. Ed.* **2018**, *57*, 769−773.
(43) Purcell, E. M.; Morin, D. J. In *Electricity and Magnetism*; Cambridge Univ. Press.: Cambridge, 2013; p 853.
(44) Evans, R.; Napper, D. H. *J. Colloid Interface Sci.* **1973**, *45*, 138−147.
(45) Dascalescu, L.; Mihailescu, M. *J. Electrost.* **1993**, *30*, 297−306.
(46) Kirsch, A. A.; Zagnit'ko, A. V. *Aerosol Sci. Technol.* **1990**, *12*, 465−470.
(47) Zheng, C.; Chang, Q.; Lu, Q.; Yang, Z.; Gao, X.; Cen, K. *Aerosol Air Qual. Res.* **2016**, *16*, 3037−3054.
(48) Pagnotti, V. S.; Inutan, E. D.; Marshall, D. D.; McEwen, C. N.; Trimpin, S. *Anal. Chem.* **2011**, *83*, 7591−7594.
(49) Hodges, M. P.; Wales, D. J. *Chem. Phys. Lett.* **2000**, *324*, 279−288.
(50) Sekimoto, K.; Takayama, M. *J. Inst. Electrostat. Jpn.* **2009**, *33*, 38−42.
(51) Sekimoto, K.; Takayama, M. *Eur. Phys. J. D* **2010**, *60*, 589−599.
(52) Sioud, S.; Kharbatia, N.; Amad, M. H.; Zhu, Z.; Cabanetos, C.; Lesimple, A.; Beaujuge, P. *Rapid Commun. Mass Spectrom.* **2014**, *28*, 2389−97.
(53) Martinez-Lozano, P.; Rus, J.; Fernandez de La Mora, G.; Hernandez, M.; Fernandez de La Mora, J. F. *J. Am. Soc. Mass Spectrom.* **2009**, *20*, 287−294.
(54) Taylor, G. B. *Ind. Eng. Chem.* **1925**, *17*, 633−635.
(55) Palma de Oliveira, D. P.; Bastos de Siqueira, M. E. P. *Quim. Nova* **2007**, *30*, 1362−1364.
(56) Baggenstoss, J.; Poisson, L.; Kaegi, R.; Perren, R.; Escher, F. *J. Agric. Food Chem.* **2008**, *56*, 5836−5846.
(57) Flament, I.; Bessière-Thomas, Y. In *Coffee Flavor Chemistry*; John Wiley & Sons: New York, 2002; p 410.

DOI: 10.1021/acs.analchem.9b00857
Anal. Chem. XXXX, XXX, XXX−XXX